OFDM SPECTRAL PRECODING WITH PER-SUBCARRIER DISTORTION CONSTRAINTS

Khawar Hussain *Roberto López-Valcarce*

atlanTTic Research Center, University of Vigo, Spain. Email: {khawar,valcarce}@gts.uvigo.es

ABSTRACT

Spectral precoding is effective in reducing out-of-band radiation (OBR) in multicarrier systems, but it introduces distortion in the data, requiring a suitable decoder at the receiver. Thus, trading off OBR reduction, implementation complexity, and error rate is of paramount importance. We present a precoder design which minimizes OBR under constraints on the distortion at each individual data subcarrier. By judiciously choosing the distortion profile, the decoding task can be significantly alleviated, with a sizable improvement in terms of implementation complexity with respect to previous designs.

***Index Terms*—** OFDM, spectral precoding, out-of-band radiation, sidelobe suppression

1. INTRODUCTION

Orthogonal frequency division multiplexing (OFDM) is a mature technology with significant advantages: it is spectrally efficient, robust against multipath effects, and well matched to multiple input multiple output (MIMO) implementation. Due to these, the Third Generation Patnership Project (3GPP) has agreed on cyclic prefix (CP)-based OFDM as the modulation technique for 5G phase 1 [1]. But OFDM also has drawbacks, such as large spectrum side lobes, causing high out-of-band radiation (OBR) and adjacent channel interference. Traditionally, OBR has been mitigated via guard-band insertion, filtering, and/or pulse shaping [2, 3]. These techniques are straightforward, but they either degrade spectral efficiency or decrease the effective CP length.

Over the years, new OBR reduction approaches have been proposed. Constellation expansion [4] and multiple choice sequences [5] require transmitting side information, causing system overhead. Subcarrier weighting [6, 7] and adaptive symbol transition techniques [8] are data dependent, i.e., they require solving an optimization problem for each OFDM symbol. Active interference cancellation (AIC) methods modulate some reserved cancellation subcarriers with appropriate data-independent linear combinations of the symbols transmitted on data subcarriers [9] [10]. AIC can be seen as a particular case of a more general family of techniques known as *spectral precoding*. A number of precoder designs have been proposed according to different criteria, e.g., smoothing the time-domain waveform [11, 12], introducing out-of-band notches [13, 14], contrast energy ratio [15], or other heuristics [16, 17, 18]. In general, these methods suffer from high complexity at both transmitter and receiver, where the precoding and decoding operations are respectively implemented.

We have recently proposed in [19] a design which trades off OBR reduction and decoder complexity by constraining the overall normalized mean squared error (NMSE) that the precoder introduces in a data block. We have observed that this *total distortion constraint* (TDC) design results in an uneven NMSE distribution among subcarriers, as shown in Fig. 1. In this example with 492 data subcarriers, the average NMSE was constrained to 0.015. As they contribute more towards OBR, edge subcarriers get more distorted than central ones. The highly distorted edge subcarriers are more prone to errors and dominate receiver complexity: the decoder needs more iterations to achieve a given error rate.

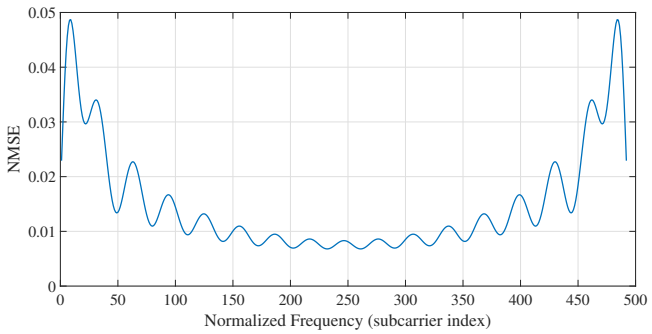

Fig. 1. Normalized MSE for the TDC design. $\epsilon_{\mathrm{TDC}} = 0.015$.

Based on these observations, and to improve on the TDC design, we explore the possibility of setting different NMSE constraints on each data subcarrier. In this way a user-selectable NMSE profile can be specified, providing more flexibility and control in the tradeoff between OBR reduction and the required number of decoder iterations. Similarly to the TDC design, the new *individual distortion constraint* (IDC) design results in precoding matrices which are approximately low rank, a property which can be exploited to further reduce complexity.

Supported by Agencia Estatal de Investigación (Spain) and the European Regional Development Fund (ERDF) under project WINTER (TEC2016-76409-C2-2-R, BES-2017-080305), and by Xunta de Galicia (Agrupación Estratéxica Consolidada de Galicia accreditation 2016-2019).

978-9-0827-9703-9/19/$31.00 ©2019 IEEE

2. SIGNAL MODEL

An N-subcarrier OFDM system with subcarrier spacing Δ_f Hz, cyclic prefix length $N_{\rm cp}$ and rectangular pulse shaping is considered. From [20], the spectrum of the kth subcarrier is $\phi_k(f) = \varphi(f/\Delta_f - k)G(f)$ for $k = 0, \ldots, N-1$, where

$$\varphi(\nu) \triangleq \frac{\sin\left(\frac{\pi(N+N_{\rm cp})\nu}{N}\right)}{\sin\left(\frac{\pi\nu}{N}\right)} \mathrm{e}^{j\pi\frac{(N+N_{\rm cp})\nu}{N}} \tag{1}$$

and $G(f)$ is the frequency response of the D/A interpolation filter, assumed here to be an ideal brickwall lowpass filter with bandwidth equal to half the sampling rate. Let $\boldsymbol{\phi}(f) = [\,\phi_0(f)\ \cdots\ \phi_{N-1}(f)\,]^T$ and $\boldsymbol{x} = [\,x_0\ \cdots\ x_{N-1}\,]^T$, with x_k the sample modulating the k-th subcarrier for a given OFDM symbol. The power spectral density (PSD) is given by

$$P_x(f) \approx \mathbb{E}\{|\boldsymbol{x}^H\boldsymbol{\phi}(f)|^2\} = \boldsymbol{\phi}^H(f)\mathbb{E}\{\boldsymbol{x}\boldsymbol{x}^H\}\boldsymbol{\phi}(f). \tag{2}$$

Assume that $N_{\rm d} \leq N$ subcarriers are allocated for data transmission, whereas a number $N_{\rm c} = N - N_{\rm d} \ll N_{\rm d}$ of cancellation subcarriers are specifically modulated to aid in OBR reduction. Let $\boldsymbol{S}$ be the $N \times N_{\rm d}$ matrix comprising the columns of $\boldsymbol{I}_N$ with indices given by the positions of data subcarriers, and let $\boldsymbol{T}$ comprise the remaining $N_{\rm c}$ columns of $\boldsymbol{I}_N$. Note, $\boldsymbol{S}^H\boldsymbol{S} = \boldsymbol{I}_{N_{\rm d}}$, $\boldsymbol{T}^H\boldsymbol{T} = \boldsymbol{I}_{N_{\rm c}}$ and $\boldsymbol{S}^H\boldsymbol{T} = \boldsymbol{0}$. Let $\boldsymbol{d}$ be the $N_{\rm d} \times 1$ data vector in the given OFDM symbol, and let $\boldsymbol{G}$ be the $N \times N_{\rm d}$ precoding matrix, so that

$$\boldsymbol{x} = \boldsymbol{G}\boldsymbol{d} = (\boldsymbol{S}\boldsymbol{P} + \boldsymbol{T}\boldsymbol{Q})\boldsymbol{d}, \tag{3}$$

where $\boldsymbol{P} = \boldsymbol{S}^H\boldsymbol{G}$ (size $N_{\rm d} \times N_{\rm d}$) and $\boldsymbol{Q} = \boldsymbol{T}^H\boldsymbol{G}$ (size $N_{\rm c} \times N_{\rm d}$). As long as $\boldsymbol{P} \neq \boldsymbol{I}_{N_{\rm d}}$, precoding will distort the data subcarriers, so that the symbol error rate will degrade unless proper compensation is applied at the receiver.

Assuming $\mathbb{E}\{\boldsymbol{d}\} = \boldsymbol{0}$ and $\mathbb{E}\{\boldsymbol{d}\boldsymbol{d}^H\} = \boldsymbol{I}_{N_{\rm d}}$, (2) becomes

$$P_x(f) \approx \mathrm{tr}\{\boldsymbol{G}^H\boldsymbol{\Phi}(f)\boldsymbol{G}\}, \qquad \boldsymbol{\Phi}(f) \triangleq \boldsymbol{\phi}(f)\boldsymbol{\phi}^H(f). \tag{4}$$

Let $\mathcal{B}$ denote the out-of-band frequency range. Defining the $N \times N$ positive (semi)definite matrices

$$\boldsymbol{A}_{\rm TOT} \triangleq \int_{-\infty}^{\infty} \boldsymbol{\Phi}(f)\,\mathrm{d}f, \qquad \boldsymbol{A}_{\rm OBR} \triangleq \int_{\mathcal{B}} \boldsymbol{\Phi}(f)\,\mathrm{d}f, \tag{5}$$

the total transmit power and OBR are respectively given by

$$P_{\rm TOT} = \int_{-\infty}^{\infty} \mathrm{tr}\{\boldsymbol{G}^H\boldsymbol{\Phi}(f)\boldsymbol{G}\}\,\mathrm{d}f = \mathrm{tr}\{\boldsymbol{G}^H\boldsymbol{A}_{\rm TOT}\boldsymbol{G}\}, \tag{6}$$

$$P_{\rm OBR} = \int_{\mathcal{B}} \mathrm{tr}\{\boldsymbol{G}^H\boldsymbol{\Phi}(f)\boldsymbol{G}\}\,\mathrm{d}f = \mathrm{tr}\{\boldsymbol{G}^H\boldsymbol{A}_{\rm OBR}\boldsymbol{G}\}. \tag{7}$$

3. PROPOSED PRECODER DESIGN

The data subcarriers are modulated by $\boldsymbol{S}^H\boldsymbol{x} = \boldsymbol{P}\boldsymbol{d} \neq \boldsymbol{d}$. With $\|\cdot\|_F$ denoting the Frobenius norm, the total NMSE is

$$\frac{\mathbb{E}\{\|\boldsymbol{P}\boldsymbol{d} - \boldsymbol{d}\|^2\}}{\mathbb{E}\{\|\boldsymbol{d}\|^2\}} = \frac{1}{N_d}\|\boldsymbol{P} - \boldsymbol{I}_{N_d}\|_F^2. \tag{8}$$

In the TDC design from [19], the constraint $\|\boldsymbol{P} - \boldsymbol{I}_{N_d}\|_F^2 \leq N_d\epsilon_{\rm TDC}$ is imposed, with $\epsilon_{\rm TDC} \geq 0$ the maximum allowable NMSE. On the other hand, with $\boldsymbol{e}_i$ the i-th column of $\boldsymbol{I}_{N_{\rm d}}$, the NMSE experienced by the i-th subcarrier is given by

$$\frac{\mathbb{E}\{|\boldsymbol{e}_i^H(\boldsymbol{P}\boldsymbol{d} - \boldsymbol{d})|^2\}}{\mathbb{E}\{|\boldsymbol{e}_i^H\boldsymbol{d}|^2\}} = \|\boldsymbol{P}^H\boldsymbol{e}_i - \boldsymbol{e}_i\|^2, \tag{9}$$

i.e., the squared Euclidean distance from $\boldsymbol{e}_i$ to the i-th *row* of $\boldsymbol{P}$. In the proposed IDC design, the NMSE (9) on each subcarrier is constrained to a maximum value $0 \leq \epsilon_i \ll 1$. The transmit power is also constrained: let $P_0 = \mathrm{tr}\{\boldsymbol{S}^H\boldsymbol{A}_{\rm TOT}\boldsymbol{S}\}$ be the transmit power for $(\boldsymbol{P}, \boldsymbol{Q}) = (\boldsymbol{I}_{N_{\rm d}}, \boldsymbol{0})$, i.e., when using null subcarriers and no precoding. The design becomes

$$\min_{\boldsymbol{P},\boldsymbol{Q}} \mathrm{tr}\{\boldsymbol{G}^H\boldsymbol{A}_{\rm OBR}\boldsymbol{G}\} \quad \text{s.to} \begin{cases} \|\boldsymbol{P}^H\boldsymbol{e}_i - \boldsymbol{e}_i\|^2 & \leq & \epsilon_i, \\ i = 1, \cdots, N_d, & & \\ \mathrm{tr}\{\boldsymbol{G}^H\boldsymbol{A}_{\rm TOT}\boldsymbol{G}\} & \leq & \beta P_0, \\ \boldsymbol{S}\boldsymbol{P} + \boldsymbol{T}\boldsymbol{Q} & = & \boldsymbol{G}, \end{cases} \tag{10}$$

where $0 < \beta \leq 1$ is a scaling factor which can be adjusted to prevent undesirable spectral spurs [21].

Problem (10) is a Least Squares (LS) problem with N_d+1 Quadratic Inequality (QI) constraints, and hence convex. Although it can be solved in principle using any suitable package, this becomes impractical as the number of subcarriers increases. This is particularly important in dynamic spectrum access systems which must reconfigure their transmission parameters as spectrum availability changes over time. Thus, we seek alternative approaches with less complexity. In particular, we note that LS problems with a *single* QI constraint (LSQI) can be efficiently solved via the Generalized Singular Value Decomposition (GSVD) [22, Ch. 12]. Our approach is to replace Problem (10) by a sequence of much simpler LSQI problems.

To this end, note first that for fixed $\boldsymbol{P}$, (10) reduces to an LSQI problem with respect to $\boldsymbol{Q}$, similarly to [19]. On the other hand, let $\widetilde{\boldsymbol{p}}_i \triangleq \boldsymbol{P}^H\boldsymbol{e}_i$, and given $\ell \in \{1, \cdots, N_d\}$, consider Problem (10) for fixed $\boldsymbol{Q}$ and $\widetilde{\boldsymbol{p}}_i$ for all $i \neq \ell$, i.e., the minimization is carried out with respect to $\widetilde{\boldsymbol{p}}_\ell$ only: in this way, an LSQI problem is obtained, whose only constraint is $\|\widetilde{\boldsymbol{p}}_\ell - \boldsymbol{e}_\ell\|^2 \leq \epsilon_\ell$. In fact, the resulting LSQI problem is highly structured and can be solved in closed form without resorting to the GSVD (details are skipped for brevity).

Based on this facts, we propose to minimize $P_{\rm OBR}$ sequentially and iteratively, first with respect to $\boldsymbol{Q}$ and then with respect to the rows of $\boldsymbol{P}$; at each step, the corresponding optimization variable is affected by a single QI constraint. The proposed iterative method is summarized in Algorithm 1.

In this way, the original problem is replaced by a sequence of easy-to-solve LSQI problems which clearly produces a sequence $(\boldsymbol{P}_k, \boldsymbol{Q}_k)$ of feasible points for problem (10). In addition, the sequence of objective values $P_{\rm OBR}(\boldsymbol{P}_k, \boldsymbol{Q}_k)$ is non-increasing and therefore convergent, since $P_{\rm OBR}$ is bounded

Algorithm 1 Precoder design with individual distortion constraints (IDC)

Initialize $k = 1$ and $\boldsymbol{P}_1 = \boldsymbol{I}_{N_d}$
repeat
  $\boldsymbol{Q}_k \leftarrow \arg\min_{\boldsymbol{Q}} P_{\mathrm{OBR}}(\boldsymbol{P}_k, \boldsymbol{Q})$ subject to $P_{\mathrm{TOT}}(\boldsymbol{P}_k, \boldsymbol{Q}) \le \beta P_0$
  $\forall\, i \in \{1, \dots, N_d\},\ \widetilde{\boldsymbol{p}}_{k,i} \leftarrow \boldsymbol{P}_k^H \boldsymbol{e}_i$
  for $\ell = 1, \dots, N_d$ **do**
    $\boldsymbol{P}_{k+1}^{(\ell)} \leftarrow \sum_{j=1}^{\ell-1} \boldsymbol{e}_j \widetilde{\boldsymbol{p}}_{k+1,j}^H + \boldsymbol{e}_\ell \widetilde{\boldsymbol{p}}_\ell^H + \sum_{j=\ell+1}^{N_d} \boldsymbol{e}_j \widetilde{\boldsymbol{p}}_{k,j}^H$
    $\widetilde{\boldsymbol{p}}_{k+1,\ell} \leftarrow \arg\min_{\widetilde{\boldsymbol{p}}_\ell} P_{\mathrm{OBR}}(\boldsymbol{P}_{k+1}^{(\ell)}, \boldsymbol{Q}_k)$ subject to $\|\widetilde{\boldsymbol{p}}_\ell - \boldsymbol{e}_\ell\|^2 \le \epsilon_\ell$
  end for
  $\boldsymbol{P}_{k+1} \leftarrow \boldsymbol{P}_{k+1}^{(N_d)}$
  $k \leftarrow k + 1$
until convergence

below. Finally, the convergent point must be feasible because the feasible set is closed.

At the receiver, after timing and carrier synchronization, the CP is discarded and an N-point FFT is applied. At its output, the samples at the N_{c} cancellation subcarriers are discarded. Channel equalization is applied to the N_{d} data subcarriers, resulting in the following $N_{\mathrm{d}} \times 1$ vector of samples:

$$\boldsymbol{r} = \boldsymbol{P}\boldsymbol{d} + \boldsymbol{w} = \boldsymbol{d} + \boldsymbol{\Delta}\boldsymbol{d} + \boldsymbol{w}, \tag{11}$$

where $\boldsymbol{w}$ is the noise vector, and $\boldsymbol{\Delta} \triangleq \boldsymbol{P} - \boldsymbol{I}_{N_{\mathrm{d}}}$ is the distortion matrix, which by design satisfies $\|\boldsymbol{\Delta}\|_F^2 \le \sum_{i=1}^{N_d} \epsilon_i$. As in [19], the fact that $\boldsymbol{\Delta}$ is small suggests the use of iterative decoding: initializing $\hat{\boldsymbol{d}}_0 = \boldsymbol{r}$, the estimate of the data vector $\boldsymbol{d}$ is obtained at iteration k as

$$\hat{\boldsymbol{d}}_k = \mathrm{DEC}\{\boldsymbol{r} - \boldsymbol{\Delta}\hat{\boldsymbol{d}}_{k-1}\}, \quad k = 1, 2, \dots \tag{12}$$

where $\mathrm{DEC}\{\cdot\}$ is an entrywise hard-decision operator, returning for each entry its closest point in the constellation.

4. COMPLEXITY ANALYSIS

It is important to quantify the implementation complexity of any OBR reduction method, both at the transmitter and the receiver. Regarding the transmitter, directly implementing (3) requires $(N_{\mathrm{d}} + N_{\mathrm{c}})N_{\mathrm{d}}$ complex multiplications per OFDM symbol (cmults/symb). However, similarly to [19], the matrices $\boldsymbol{\Delta}$ and $\boldsymbol{Q}$ obtained with the proposed IDC design happen to be approximately low-rank. Thus, their respective SVDs can be truncated to their $r_\Delta \ll N_{\mathrm{d}}$ and $r_Q \ll N_{\mathrm{d}}$ principal components, yielding accurate approximations of the form

$$\boldsymbol{\Delta} \approx \boldsymbol{L}_\Delta \boldsymbol{R}_\Delta^H, \qquad \boldsymbol{Q} \approx \boldsymbol{L}_Q \boldsymbol{R}_Q^H, \tag{13}$$

where $\boldsymbol{L}_\Delta$, $\boldsymbol{R}_\Delta$ have size $N_{\mathrm{d}} \times r_\Delta$, whereas $\boldsymbol{L}_Q$ and $\boldsymbol{R}_Q$ respectively have size $N_{\mathrm{c}} \times r_Q$ and $N_{\mathrm{d}} \times r_Q$. Then the transmitter computes $\boldsymbol{P}\boldsymbol{d} \approx \boldsymbol{d} + \boldsymbol{L}_\Delta(\boldsymbol{R}_\Delta^H \boldsymbol{d})$ and $\boldsymbol{Q}\boldsymbol{d} \approx \boldsymbol{L}_Q(\boldsymbol{R}_Q^H \boldsymbol{d})$, requiring only $2r_\Delta N_{\mathrm{d}} + r_Q(N_{\mathrm{d}} + N_{\mathrm{c}})$ cmults/symb.

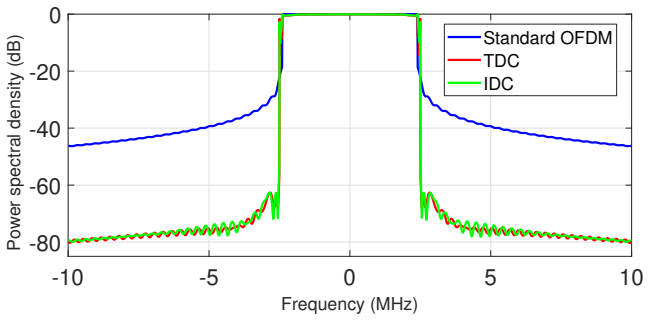

Fig. 2. Obtained PSDs for a system with $N = 512$, $N_{\mathrm{c}} = 20$. "Standard OFDM" refers to a system with $(\boldsymbol{P}, \boldsymbol{Q}) = (\boldsymbol{I}_{N_d}, \boldsymbol{0})$.

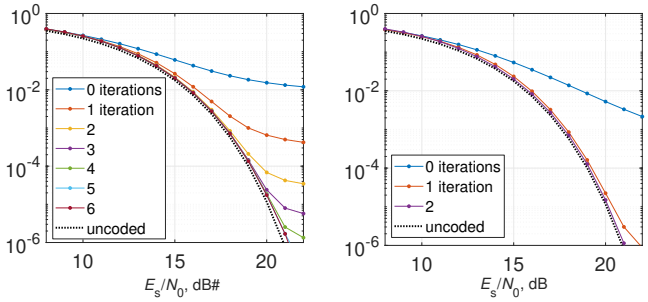

Fig. 3. SER in AWGN channel, $N = 512$, $N_{\mathrm{c}} = 20$. TDC design (left), IDC design (right).

On the other hand, receiver complexity is dominated by the product $\boldsymbol{\Delta}\hat{\boldsymbol{d}}_{k-1}$ in (12). If the total number of decoding iterations is N_{it}, then direct implementation of such product results in $N_{\mathrm{d}}^2 N_{\mathrm{it}}$ cmults/symb. Using (13) instead, this is reduced to $2r_\Delta N_{\mathrm{d}} N_{\mathrm{it}}$ cmults/symb. N_{it} will depend on the distortion present in the precoded signal, resulting in a tradeoff between OBR reduction and decoding complexity as in the TDC design from[19]. However, the fact that the IDC design allows to fine-tune the distortion level on a per-subcarrier basis results in a more favorable tradeoff, as shown next.

5. NUMERICAL EXAMPLES

We compare the proposed IDC design with previous schemes, in terms of OBR reduction, symbol error rate (SER), and implementation complexity. In the following numerical examples we consider a CP-OFDM system carrying 16-QAM data, with 5 MHz bandwidth, $N = 512$ subcarriers and $1/32$ CP. The sampling rate of the D/A converter is 20 MHz, so that $\mathcal{B} = [-10, -2.5] \cup [2.5, 10]$ MHz.

In the first example, the IDC and TDC designs are compared for $N_{\mathrm{d}} = 492$, so that 10 cancellation subcarriers are reserved at each spectrum edge. To have similar behavior in terms of spectral overshoot, the values $\beta_{\mathrm{TDC}} = 0.974$ and $\beta_{\mathrm{IDC}} = 0.98$ were chosen. The average NMSE in the TDC

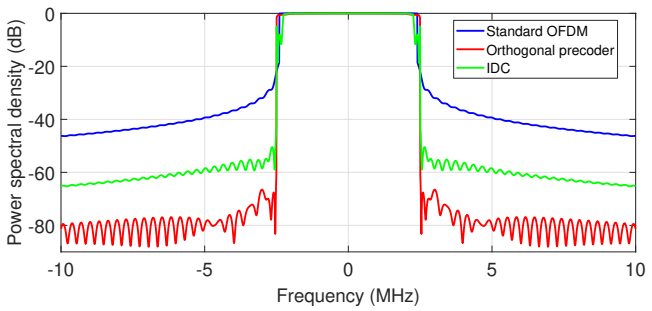

Fig. 4. Obtained PSDs for a system with $N = 512$, $N_c = 50$.

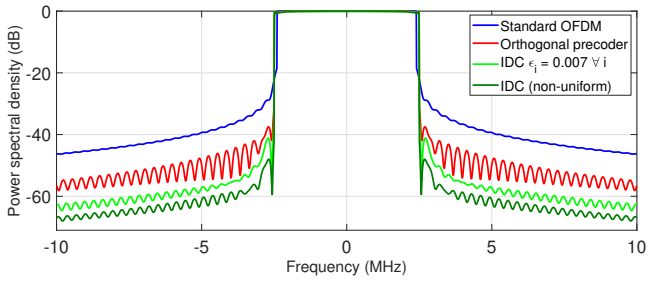

Fig. 5. Obtained PSDs for a system with $N = 512$, $N_c = 4$.

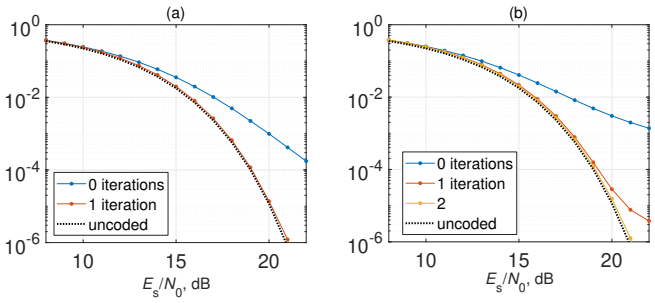

Fig. 6. SER in AWGN channel of the proposed iterative decoder with IDC design. (a) $\epsilon_i = 0.007\ \forall i$, (b) ϵ_i as in Fig. 7.

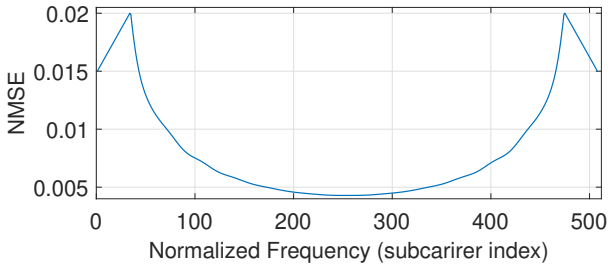

Fig. 7. Distortion profile $\{\epsilon_i\}$ of the proposed IDC design.

design was set to $\epsilon_{\text{TDC}} = 0.015$, whereas for IDC the NMSE at each data subcarrier was set to $\epsilon_i = 0.013$. These values yield similar results in terms of OBR, as seen in Fig. 2. Fig. 3 shows the SER of both designs in an AWGN channel. The proposed IDC design requires fewer decoder iterations (about 2) to cover the gap to the uncoded system, whereas the TDC design needs 5 iterations to do so. For both TDC and IDC, the resulting matrices $\boldsymbol{\Delta}$ (size 492×492) and $\boldsymbol{Q}$ (size 20×492) were replaced by their best low-rank approximations with $(r_\Delta, r_Q) = (12, 7)$, without compromising performance. With this, both precoders required $15,392$ cmults/symb. The decoder complexities for TDC ($N_{\text{it}} = 5$) and IDC ($N_{\text{it}} = 2$) are $59,040$ and $23,616$ cmults/symb, respectively. Receiver complexity is thus reduced by 60%.

The IDC design is flexible enough to meet different system requirements. In the second example, the number of cancellation subcarriers is $N_c = 50$ out of $N = 512$. Fig. 4 shows the PSDs obtained by the proposed method (with $\beta_{\text{IDC}} = 1$ and $\epsilon_i = 0.003$ for all i) and the orthogonal precoder design from [15]. Although IDC is outperformed in terms of OBR reduction, it still provides satisfactory performance at only a fraction of the cost. Using $(r_\Delta, r_Q) = (5, 8)$, a single iteration suffices at the decoder, yielding 8,716 and 4,620 cmults/symb respectively at the transmitter and receiver. In contrast, even when using the low-complexity implementation from [23], the orthogonal precoder requires 48,700 cmults/symb at both transmitter and receiver.

In the third example we consider a bandwidth-limited scenario with only $N_c = 4$ cancellation subcarriers available. In this case, the orthogonal precoder requires 4,080 cmults/symb at both transmitter and receiver. The OBR reduction obtained by orthogonal precoding can be improved if one uses IDC precoding instead, at the cost of additional complexity. Fig. 5 shows an example with $\beta_{\text{IDC}} = 0.983$, $\epsilon_i = 0.007\ \forall i$. In this case, the decoder requires a single iteration, see Fig. 6(a). Using $(r_\Delta, r_Q) = (7, 4)$, the complexity incurred is 9,160 and 7,112 cmults/symb at the transmitter and receiver, respectively.

Moreover, with the IDC design it becomes possible to further improve the performance by judiciously specifying a non-uniform NMSE profile $\{\epsilon_i\}$. In particular, using the profile shown in Fig. 7, the OBR is further reduced by more than 6 dB as seen in Fig. 5, with the same values $(r_\Delta, r_Q) = (7, 4)$, and one additional decoder iteration, see Fig. 6(b).

6. CONCLUSION

The proposed spectral precoder design has manageable off-line complexity, and provides significant flexibility when achieving a tradeoff between out-of-band radiation reduction and on-line computational complexity. The fact that the maximum distortion experienced by data subcarriers can be specified on a per-subcarrier basis can be exploited in order to reduce the number of iterations required by the decoder, significantly reducing the computational complexity of the receiver. In this way, system requirements can be met in a broad variety of settings. Future research will address the optimization of the per-subcarrier distortion profile.

7. REFERENCES

[1] Group Radio Access Network, "TS38.211: NR; Physical channels and modulation (Release 15)," https://portal.3gpp.org/desktopmodules/Specifications/SpecificationDetails.aspx?specificationId=3213, Mar. 2018.

[2] X. Huang, J. A. Zhang, and Y. J. Guo, "Out-of-band emission reduction and a unified framework for precoded OFDM," *IEEE Commun. Mag.*, vol. 53, no. 6, pp. 151–159, Jun. 2015.

[3] M.-F. Tang and B. Su, "Joint window and filter optimization for new waveforms in multicarrier systems," *EURASIP J. Adv. Signal Process.*, vol. 2018, no. 1, pp. 63–82, Oct. 2018.

[4] S. Pagadarai, R. Rajbanshi, A. M. Wyglinski, and G. J. Minden, "Sidelobe suppression for OFDM-based cognitive radios using constellation expansion," in *IEEE Wireless Commun. Netw. Conf.*, 2008, pp. 888–893.

[5] I. Cosovic and V. Janardhanam, "Sidelobe suppression in OFDM systems," in *Multi-Carrier Spread-Spectrum*, K. Fazel and S. Kaiser, Eds., Dordrecht, 2006, pp. 473–482, Springer Netherlands.

[6] I. Cosovic, S. Brandes, and M. Schnell, "Subcarrier weighting: a method for sidelobe suppression in OFDM systems," *IEEE Commun. Lett.*, vol. 10, no. 6, pp. 444–446, Jun. 2006.

[7] R. Kumar and A. Tyagi, "Extended subcarrier weighting for sidelobe suppression in OFDM based cognitive radio," *Wireless Pers. Commun.*, vol. 87, no. 3, pp. 779–796, Apr. 2016.

[8] H. A. Mahmoud and H. Arslan, "Sidelobe suppression in OFDM-based spectrum sharing systems using adaptive symbol transition," *IEEE Commun. Lett.*, vol. 12, no. 2, pp. 133–135, Feb. 2008.

[9] S. Brandes, I. Cosovic, and M. Schnell, "Reduction of out-of-band radiation in OFDM systems by insertion of cancellation carriers," *IEEE Commun. Lett.*, vol. 10, no. 6, pp. 420–422, Jun. 2006.

[10] J. F. Schmidt, S. Costas-Sanz, and R. López-Valcarce, "Choose your subcarriers wisely: Active interference cancellation for cognitive OFDM," *IEEE J. Emerg. Sel. Topics Circuits Syst.*, vol. 3, no. 4, pp. 615–625, Dec. 2013.

[11] J. van de Beek and F. Berggren, "N-continuous OFDM," *IEEE Commun. Lett.*, vol. 13, no. 1, pp. 1–3, Jan. 2009.

[12] M. Mohamad, R. Nilsson, and J. van de Beek, "Minimum-EVM N-continuous OFDM," in *IEEE Int. Conf. Commun.*, May 2016, pp. 1–5.

[13] J. van de Beek, "Sculpting the multicarrier spectrum: a novel projection precoder," *IEEE Commun. Lett.*, vol. 13, no. 12, pp. 881–883, Dec. 2009.

[14] J. Zhang, X. Huang, A. Cantoni, and Y. J. Guo, "Sidelobe suppression with orthogonal projection for multicarrier systems," *IEEE Trans. Commun.*, vol. 60, no. 2, pp. 589–599, Feb. 2012.

[15] R. Xu and M. Chen, "A precoding scheme for DFT-based OFDM to suppress sidelobes," *IEEE Commun. Lett.*, vol. 13, no. 10, pp. 776–778, Oct. 2009.

[16] C.-D. Chung, "Correlatively coded OFDM," *IEEE Trans. Wireless Commun.*, vol. 5, no. 8, pp. 2044–2049, Aug. 2006.

[17] C.-D. Chung, "Spectrally precoded OFDM," *IEEE Trans. Commun.*, vol. 54, no. 12, pp. 2173–2185, Dec. 2006.

[18] X. Zhou, G. Y. Li, and G. Sun, "Low-complexity spectrum shaping for OFDM-based cognitive radio systems," *IEEE Signal Process. Lett.*, vol. 19, no. 10, pp. 667–670, Oct. 2012.

[19] K. Hussain, A. Lojo, and R. López-Valcarce, "Flexible spectral precoding for sidelobe suppression in OFDM systems," in *IEEE Int. Conf. Acoust., Speech, Signal Process.*, 2019, accepted.

[20] T. van Waterschoot, V. Le Nir, J. Duplicy, and M. Moonen, "Analytical expressions for the power spectral density of CP-OFDM and ZP-OFDM signals," *IEEE Signal Process. Lett.*, vol. 17, no. 4, pp. 371–374, Apr. 2010.

[21] J. F. Schmidt and R. López-Valcarce, "OFDM spectrum sculpting with active interference cancellation: Keeping spectral spurs at bay," in *IEEE Int. Conf. Acoust., Speech, Signal Process.*, May 2014, pp. 8053–8057.

[22] G. H. Golub and C. F. Van Loan, *Matrix Computations (3rd Ed.)*, Johns Hopkins University Press, Baltimore, MD, USA, 1996.

[23] I. V. L. Clarkson, "Orthogonal precoding for sidelobe suppression in DFT-based systems using block reflectors," in *IEEE Int. Conf. Acoust., Speech, Signal Process.*, 2017, pp. 3709–3713.